Published in final edited form as:
Nanotechnology. 2011 April 1; 22(13): 135102. doi:10.1088/0957-4484/22/13/135102.

Synthesis and Bioevaluation of ^{125}I-Labeled Gold Nanorods

Xia Shao[1], **Ashish Agarwal**[2], **Justin R. Rajian**[1], **Nicholas A. Kotov**[2], and **Xueding Wang**[1,*]

[1] Department of Radiology, University of Michigan, Ann Arbor, MI

[2] Department of Chemical Engineering, University of Michigan, Ann Arbor, MI 48103, USA

Abstract

A novel technique is discribed to monitor *in vivo* behaviors of gold nanorods (GNRs) using γ-imaging. GNRs were radiolabeled using [^{125}I] sodium iodide in a simple and fast manner with high yield and without disturbing optical properties. Radiolabeled GNRs were successfully visualized by radioisotope tag, allowing longitudinal in vivo studies to be performed repeatedly in the same animal. The preliminary biodistribution study showed that PEGylated GNRs have much longer blood circulation times and clear out faster, while bare GNRs accumulate quickly in the liver after systematic administration. The highly efficient method reported here provides an extensively useful tool for guidance of design and development of new gold nanoparticles as target-specific agents for both diagnostics and photothermal therapy.

Keywords

Gold nanorods; Iodine-125; γ-imaging; Radiolabeled nanoparticles; PEGylation

1. Introduction

Nanoparticles, due to their small sizes and associated unique properties, have been widely used in drug delivery (1–4), cellular imaging (5–9), and biomedical diagnostics and therapeutics (10–13). Plasmonic gold nanostructures possess intriguing physical and chemical properties which are of interest to both fundamental science and biomedical application (14). Among the most fascinating and useful are optical properties as well as related photothermal properties (15). These optical properties depend on nanoparticle size and shape (16, 17). One can manipulate the shape of gold nanostructures to control their electronic and associated optical properties for different desired applications (18, 19). Their remarkable capacity to absorb and scatter light at visible and near-infrared (NIR) regions is essential for optical imaging (20). In addition, gold nanoparticles can convert optical energy into heat via nonradiative electron relaxation dynamics which endows them with intense photothermal properties (21–24). Such localized heating effects can be directed toward the eradication of diseased tissue, providing a noninvasive alternative to surgery (25). Current nanotechnology research suggests that gold nanoparticles form a novel class of optically active dual imaging-therapy agents (26–28).

In particular, gold nanorods (GNRs) have attracted much interest because of their small sizes, ease of preparation and bioconjugation, strong absorbing and scattering properties, as well as their well-known biocompatibility (14, 20, 29, 30). GNRs with well-defined shapes and sizes are readily synthesized by seeded growth methods, and their longitudinal plasmon resonances (LPRs) can be finely tuned as a function of aspect ratio (14, 29, 31). GNRs

*To whom correspondence should be addressed. xdwang@umich.edu.

support a larger absorption cross-section at NIR frequencies per unit volume than most other nanostructures and have narrower line widths due to reduced radiative damping effects with consequently higher optothermal conversion efficiencies (20, 21, 32). The LPRs can also support nonlinear optical effects, such as plasmon-enhanced two-photon luminescence (TPL) (20, 33). The LPRs are also sensitive to the polarization of the incident excitation; by slightly adjusting the wavelength of a continuous-wave (cw) polarized laser, individual GNRs can be aligned for several minutes in an optical trap (34). These properties give rise to many exciting possibilities to deploy GNRs for biological imaging and photothermal therapy (20). Furthermore, the surface chemistry of GNRs allows multiple functionalizations. Capping molecules, such as cetyltrimethylammonium bromide (CTAB), can be replaced or conjugated with many functional groups (35–37). Target specificity of GNRs can be imparted by tagging with certain biovectors, such as monoclonal antibodies (38), receptor-specific peptides (14) and other compounds (20, 39), which can navigate them to desired organs or sites. Recent studies have successfully demonstrated that GNRs with strong near-IR absorption can be conjugated to molecules to facilitate delivery to the tumor for subsequent efficient cancer cell diagnostics and selective photothermal therapy simultaneously (14, 30, 38).

In addition, the techniques of introducing polyethylene glycol (PEG) to the surface of nanoparticles allow steric stabilization of particles. Polyethylene glycol can shield nanoparticles from fouling by serum proteins and reduce the adsorption of reticuloendothelial system (RES) factors in the blood to the particle surface. This reduces the rate of clearance of particles by cell of monophagocytic system and creates long-circulating particles, which hold the promise to *in vivo* utilizations of nanoparticles.

To advance GNRs toward realistic clinical applications and to optimize their diagnostic sensitivity, payload, or therapeutic efficiency, it is becoming urgent to understand how they interact with biological systems. Various *in vitro* studies have provided fundamental information as to how nanoparticle size and surface chemistry greatly impact their interaction with plasma proteins, cellular uptake, toxicity, and molecular response. However, the in vivo environment is far more complex than in vitro model systems (38–41). For instance, blood contains a variety of ions such as hydrogen, Na, Cl, Ca, etc., as well as proteins, lipids, hydrocarbons, and other components that may affect nanoparticle stability and functionality (38). Studying the stability and functionality of injected GNRs within the *in vivo* environment is technically challenging.

Recently, there are increasing utilizations of radioisotopes to study nanoparticles due to high sensitive detection of radioactivity. In most cases, a bifunctional group, like 1,4,7,10-tetraazadodecane-*N*,*N*’,*N*”,*N*’”-tetraacetic acid (DOTA), has to be conjugated to the nanoparticle and then a radioactive metal needs to be attached. These require modification of nanoparticles before radiolabeling. The study we report here is the initial investigation of the *in vivo* behavior of [^{125}I]-iodine labeled gold nanorods, which uses I-125 directly labeling gold nanorods. It has been proven that iodide ions showed high affinity and strong binding to the surface of gold nanorods (44, 45, 46). [^{125}I]-iodine should be easily tagged onto GNRs by simple mixing. The labeling method developed here can be adopted to I-123, I-124, and I-131 for more extensive applications. The stability and metabolism pattern of radiolabeled GNRs in normal rats were successfully examined using γ-scintigraphy. Longitudinal biodistribution studies have been performed repeatedly in the same animal for up to 6 days, therefore decreasing sources of inter-individual variation while being efficient in terms of animal cost and ethical practice. Radiolabeling of GNRs allows systematic study of gold nanoparticles within *in vitro* and *in vivo* microenvironments, providing a highly efficient methodology for bioevaluation of different kinds of GNRs and their bioconjugates.

The novel protocol reported here could be extensively useful for guidance of the design and the development of new target-specific gold nanoparticles.

2. Materials and methods

2.1. Materials

[^{125}I]Radionuclide in 10^{-5}M NaOH (pH 8–11) was purchased from PerkinElmer with specific activity of 100 mCi/mL. Fresh deionized water was used to dilute [^{125}I]NaI upon activity desired, around 3 mCi/mL for animal studies. Chemicals and solvents were purchased from Sigma-Aldrich (Milwaukee, WI) or Fisher Scientific (Fair Lawn, NJ) and used without further purification.

2.2. Synthesis of PEGylated Gold Nanorods

GNRs of average aspect ratio 4, capped with hexadecyltrimethyl ammonium bromide were synthesized using the seed-mediated growth methods reported in the literatures (42, 43). After synthesis gold nanorods were centrifuged and redispersed in deionized water to a final concentration of 10^{12} rods/mL. Polyethylene glycol thiol molecules were dispersed in deionized water (1ml, 50mg/mL) and mixed with GNRs (1ml, 10^{12} rods/mL). The mixture was allowed to react overnight, followed by centrifugation and redispersion of rods to a final concentration of 10^{12} rods/mL. The zeta potential of bare gold nanorods is +40mV and after PEGylation is reduced to +8mV (5000 mol. wt.) and +10 mV (20,000 mol. wt.)

2.3. Radiolabeling of Gold Nanorods

In general, 0.1 mL of GNRs with concentration of 10^{12} rods/mL in deionized water was placed into a polypropylene microcentrifuge tubes (1.5 mL) and 0.5 mL of diluted [^{125}I]NaI was added, roughly 300 μCi of radioactivity. The vial was rotated on a ROTAMIX rotates (Appropriate Technical Resources, Inc. Laurel, MD). The mixture was then centrifuged at 5000 rpm using a Beckman Microfuge II. The supernatant was decanted and pellets were re-dispersed in 0.1 mL of fresh sterile filtered deionized water. Various reaction times of 2, 10, 20, and 30 minutes have been tested, as well as various centrifugation periods of 5, 10, 15 and 30 minutes. The optical absorption spectra of diluted GNRs in saline solution were measured before and after radiolabeling by using a spectrophotometer (Perkin Elmer, MA, USA) with the sample contained in a 1 cm pathlength plastic cuvette. GNRs were also imaged by transmission electron microscopy (TEM).

2.4. Stability of gold nanorods in blood circulation

Male Sprague-Dawley rats (~250g) were purchased from Charles River Laboratories (Wilmington, MA). The rats were anesthetized using an isoflurane anesthesia machine. Two I.V. catheters were placed into lateral tail veins separately, one for injection of the ^{125}I-GNRs dose and another for extraction of blood samples. The catheters were rinsed with 0.2 mL of saline after injection and every extraction. ^{125}I-labeled gold nanorods prepared as mentioned above were injected into rats through a tail vein, 100 ~ 130 μCi in 0.1 mL of water for each animal. Three rats were used for each kind of GNRs. Blood samples (0.1 mL) were collected from another tail vein at set times, from 1 minute to 4 hour post-injection. Radioactivity in each blood sample was counted using a γ-counter (MINAXI Auto-gamma 5000 Series, Packard Instrument Co., Grove, IL).

2.5. Long-term biodistribution using γ-imaging

The same group of animals used for blood assays were imaged at set times between blood sampling. After the measurements in day 1, the animals were re-anesthetized and scanned once each day from day 2 to day 6 before they were sacrificed. Each image was acquired in

5-minute on an anesthetized rat placed in anterior position over the parallel-hole collimator 1.8/0.2/20 (Hole diameter/septum thickness/height in mm) of a Gamma Imager (Biospace Lab, Paris). Radioactivity was then quantified by drawing regions of interest (ROI) using Gamma Vision+ software (Version 3.0). For each animal, ROIs were drawn around the liver/spleen and heart/lung and were saved to be re-used systematically for longitudinal follow-up.

3. Results

3.1. Preparation of ^{125}I-labeled Gold Nanorods

GNRs either bare or PEGylated were radiolabeled by mixing with [^{125}I] sodium iodide in deionized water at room temperature. The reaction takes place very rapidly and completely, with radiochemical yield greater than 90% by radioactivity count and specific activity greater than 5×10^5 Ci/mmol. No differences in yield and specific activity were noticed between bare GNRs and PEGylated GNRs. There were no significant differences observed when the mixtures of [^{125}I] sodium iodide and GNRs were mixed for 2, 10, 20, or 30 minutes prior to centrifugation. This agrees well with the prior reports of high affinity and strong binding of iodide ions to the surface of gold nanorods (44, 45, 46). It has previously been reported that iodide ions may affect the shape and size of GNRs (45). In our case, the concentration of iodide is extremely low and has no significant impact on the optical property of GNR. Figure 1 shows the absorption spectra of GNRs measured before and after radiolabeling in a wavelength range from 400 to 1000 nm. Both transverse and longitudinal plasmon peaks remain unchanged in intensity after radiolabeling but show a small plasmon shift due to presence of additional iodine molecules on the surface. [^{125}I]-iodine labeled GNRs are stable for weeks when stored in the refrigerator.

The images of transmission electron microscopy (TEM) are shown in Figure 2. The shape and size of GNRs remains unchanged before and after radiolabeling. There are no differences observed from bare, 5K and 20K PEGylated GNRs.

The washing process using centrifugation is critical. Uncompleted centrifugation causes loss of radioactive GNRs in decanted supernatant, resulting in low radiochemical yields. On the other hand, the chance of irreversible nanorod aggregation increases when centrifugation period is extended. A series of experiments were performed to investigate and optimize the conditions. To minimize variations, radiolabeled GNRs were initially washed twice to remove free radioactive iodide and then dispersed in deionized water. Table 1 summarizes the percentage of radioactivity collected in pellets after centrifugation for various time periods. It should be noticed that a centrifugation time of 30 minutes at 5000 rpm is necessary to recover all GNRs. However, the possibility of failure to deliver desired product would then be over 30% due to irreversible nanorod aggregation. Therefore, one washing using 15 minutes centrifugation was applied for subsequent animal studies. No further washing will be needed due to high affinity of iodide ions to GNRs.

In summary, injectable doses for animal studies were prepared by mixing 0.5 mL of [^{125}I] sodium iodide with desired activity and 0.1 mL of GNRs (10^{12} rods/mL) for 5 minutes, and then centrifuging at 5,000 rpm for 15 minutes. The supernatant was decanted and pellets were re-dispersed in 0.1 mL of fresh sterile filtered deionized water. The same procedure was applied for bare, 5K and 20K PEGylated GNRs.

3.2. Stability of gold nanorods in blood circulation

To determine the circulating time of gold nanorods, we assayed blood samples from rats (n=3 for each kind of GNRs) using γ-scintigraphy. The time-activity curves are shown in Figure 3, and indicate significant differences between bare GNRs and PEGylated GNRs.

Injected bare GNRs were cleared out from blood circulation within 10 minutes, while greater than 50% of PEG coated GNRs remained in the blood after 4 hours. This is in good agreement with previous studies which have shown that a surface brush layer of PEG reduces the adsorption of blood RES factors to the particle surface hence decreasing the rate of particle clearance (40, 49). We have also found that it is irrelevant whether 5,000 or 20,000 molecular weight is used.

3.3. Long-term biodistribution using γ-imaging

The next experiment evaluated the relatively long-term biodistribution in rat for up to 6 days using γ-imaging. The same group of animals (n=3 for each kind of GNRs) used for blood assays were imaged at set times between blood sampling. Each image was acquired in 5-minute on an anesthetized rat placed in anterior position over the parallel-hole collimator of a Gamma Imager. Radioactivity was then quantified by drawing regions of interest (ROI). For each animal, ROIs were drawn around the liver/spleen and heart/lung and were saved to be re-used systematically for longitudinal follow-up. Figure 4 shows typical rat gamma images.

The linearity and precision of gamma detection were determined by scanning a series of standards with known radioactivities. The standards were prepared by serial dilution of a ^{125}I-GNRs injection sample. To obtain the average and the standard deviation, each standard was imaged 8 times in various positions over the parallel-hole collimator, each taking 5-minute for acquisition. Radioactivity was then quantified by drawing regions of interest around the standard. Figure 5 shows good correlation between radioactivities counted by a Capintec and radioactivities measured by scintigraphic acquisition of the Gamma Imager. The coefficient of determination (R^2) value was greater than 0.99. The exact position of the sample on the camera head was shown to be irrelevant.

Radioactivities in liver/spleen and heart/lung determined by the Gamma Imager were converted to injection dose based on this standard curve. The uptakes of liver/spleen and heart/lung were then normalized to % of the injected dose for each animal. Results are shown in Figure 6.

Uncoated bare gold nanorods were found accumulated quickly in the liver and spleen area within 5 minutes. It should be noted that, for bare gold nanorods, radioactivity was retained in the liver and spleen for days. The radioactivity was well represented the concentration of gold nanorods because any disassociated I-125 should be collected in thyroid. In contrast, PEG coated gold nanorods remained in the blood pool for much longer period, but the long term accumulation was minimal in liver and spleen area.

All animals were sacrificed at day 6 and examined. There was no apparent damage observed in heart, lung and liver. Thyroids of all animals had radioactivity as expected. PEG coated gold nanorods gave higher thyroid uptake, while bare rods had been trapped in liver from earlier time point and not much free iodide get into thyroid. To keep all animals in the same condition, we did not pre-treat any rats with cold iodine to block thyroid at this experiment.

4. Discussion

To date, there has been no previously reported *in vivo* animal study using I-125 labeled gold nanorods. We have optimized the radiolabeling procedures, facilitating reproducible and reliable production of injectable doses for animal studies. GNRs were successfully visualized by iodine-125 tag allowing highly sensitive detection. This simple setup can be further developed to deliver injectable dose for clinical application.

The stability of injected GNRs within body is a key issue for successful targeting of GNRs because they must be able to circulate in the blood long enough to find their targets (38). However, the reticuloendothelial system (RES) of the body filters nanoparticles from blood circulation based on their size and surface characteristics (20, 40). Rapid clearance of nanoparticles from blood limits their targeting capabilities. Polyethylene glycol (PEG) has well-established “stealth” properties that can shield nanoparticles from fouling by serum proteins (opsonization) and reduce their rate of clearance by the RES (20, 47). The beneficiary effects of PEGylation on the clearance time of injected nanoparticles have been demonstrated (38, 48). Therefore, we synthesized three different kinds of GNRs, normal bare GNR, PEGylated GNR with PEG 5,000 (mw) and PEG 20,000, and examined their stabilities in blood circulation. The preliminary animal results are very promising. Significant differences between bare GNRs and PEGylated GNRs have been observed with minimum amount of animal used (Fig. 3). PEG coated GNRs remained in the blood much longer than bare GNRs. This provided evidences that a surface brush layer of PEG reduces the adsorption of blood RES factors to the particle surface hence decreasing the rate of particle clearance (40, 49). The blood assay method described above is easy and reliable, providing initial information of novel gold nanorods in biosystems. The γ-scintigraphy is highly sensitive. Only a low dose of radioactivity has to be administrated and a small amount of blood sample needs to be drawn for measurement. This simple assay would be the first step for screening any newly designed target-specific GNRs.

The linearity and precision of Gamma Imager were tested by scanning a series of standards with known radioactivities. The coefficient of determination (R^2) value was greater than 0.99 (Fig. 5), indicating accurate and reliable measurement. For long-term biodistribution study, the liver/spleen and heart/lung areas were chosen as regions of interest because GNR particles accumulate in the liver and spleen when they are removed from blood; while they can be seen in the heart and lung when they are still freely circulating in the blood. Figure 6 shows the significant differences of uptakes between bare GNRs and PEGylated GNRs, and more importantly, the distinct metabolism pattern. The bare gold nanorods were retained in the liver and spleen for days. This indicates that bare metal particles are cleared from the body with difficulty. In contrast, PEG coated gold nanorods remained in the blood pool for much longer period, but the long term accumulation was minimal in liver and spleen area. For both the measurements form the heart/lung and liver/spleen areas, there is no noticeable difference between the results from the GNRs coated with PEG 5,000 and PEG 20,000. The observed efficient metabolism clearance pattern provides evidence that PEGylated gold nanorods are more biocompatible within the body. They are hence ideal candidates for target-specific duel agents for diagnostics and selective photothermal therapy. The trends described here need to be tested in more detail with a wider range of gold nanorods and will be reported in due course. This methodology provides a highly efficient tool for monitoring *in vivo* behaviors of gold nanoparticles.

In addition, we have successfully utilized gold nanorods to enhance the contrast in photoacoustic tomography (PAT) (31). We expect that radioisotope labeled gold nanorods can lead to the development of dual-modality imaging with the combination of nuclear imaging, like SPECT or PET, and PAT. Furthermore, it is hopeful that radiolabeled gold nanorods will become an efficient therapy agent with the combination of the power of radiation therapy and photothermal therapy.

5. Conclusion

PEGylated gold nanorods are ideal candidates for target-specific duel agents for diagnostics and selective photothermal therapy. The methodology developed here should provide a highly efficient protocol for monitoring *in vivo* behaviors of gold nanoparticles.

Longitudinal biodistribution studies have been performed repeatedly in the same animal, therefore decreasing sources of inter-individual variations and also being beneficial in terms of animal cost and ethical practice. With this powerful tool in hand, more work can be done to advance gold nanorods technology to a level for clinical use in regards to clearance, safety, efficacy of deliverance and targeting. Encouraged by the preliminary study reported here, further investigations of GNRs with various sizes, shapes, and different conjugates are investigation. Radiolabeled gold nanorods hold promise to enable the development of multifunctional nonamedical platforms for simultaneous targeting, imaging, and therapy administration.

Acknowledgments

This work was supported by National Institutes of Health grant R01 AR055179. We thank Phillip Sherman and Carole Quesada for their assistance with the animal studies.

References

1. Rawat M, Singh D, Saraf S. Biol Pharm Bull. 2006; 29:1790–1798. [PubMed: 16946487]
2. Petrak K. J Biomater Sci Polym Ed. 2006; 17:1209–1219. [PubMed: 17176746]
3. Rabinow B, Chaubal M. Drugs Pharm Sci. 2006; 159:199–229.
4. Chavanpatil MD, Khdair A, Panyam J. J Nanosci Nanotechnol. 2006; 6:2651–2663. [PubMed: 17048473]
5. Hayat, MA. Van Nostrand Reihold. New York: 1970.
6. Bruchez M Jr, Moronne M, Gin P, Weiss S, Alivisatos AP. Science. 1998; 281:2013–2016. [PubMed: 9748157]
7. Chan WCW, Nie S. Science. 1998; 281:2016–2018. [PubMed: 9748158]
8. Wu X, Liu H, Liu J, Haley KN, Treadway JA, Larson JP, Ge N, Peale F, Bruchez MP. Nat Biotechnol. 2003; 21:41–46. [PubMed: 12459735]
9. Sanstra S, Dutta D, Walter GA, Moudgil BM. Technol Cancer Res Treat. 2005; 4:593–602. [PubMed: 16292879]
10. Brigger I, Dubernet C, Couvreur P. Adv Drug Deliver Rev. 2002; 54:631–651.
11. Holm BA, Bergey EJ, De T, Rodman DJ, Kapoor R, Levy L, Friend CS, Prasad PN. Mol Cryst Liq Cryst. 2002; 374:589–598.
12. Moghimi SM, Hunter AC, Murray JC. FASEB J. 2005; 19:311–330. [PubMed: 15746175]
13. Jain KK. Clin Chim Acta. 2005; 358:37–54. [PubMed: 15890325]
14. Oyeler AK, Chen PC, Huang X, El-Sayed IH, El-Sayed MA. Bioconjugate. 2007; 18:1490–1497.
15. Zhang JZ. The J of Phys Chem Lett. 2010; 1:686–695.
16. El-Sayed MA. Acc Chem Res. 2001; 34:257–264. [PubMed: 11308299]
17. Kelly KL, Coronado E, Zhao L, Schatz GC. J Phys Chem B. 2003; 107:668–677.
18. Sun Y, Xia Y. Anal Chem. 2002; 20:5297–5305. [PubMed: 12403584]
19. Noguez C. J Phys Chem B. 2007; 111:3806–3819.
20. Tong L, Wei Q, Wei A, Cheng J. Photochem and Photobio. 2009; 85:21–32.
21. Chou C-H, Chen C-D, Wang CRC. J Phys Chem. 2005; 109:11135–11138.
22. Petrova H, Juste JP, Pastoriza-Santos I, Hartland GV, Liz-Marzan LM, Mulvaney P. Phys Chem Chem Phys. 2006; 8:814–821. [PubMed: 16482322]
23. Hirsch LR, Stafford RJ, Bankson JA, Sershen SR, Rivera B, Price RE, Hazle JD, Halas NJ, West JL. Proc Natl Acad Sci USA. 2003; 100:13549–13554. [PubMed: 14597719]
24. O'Neal DP, Hirsch LR, Halas NJ, Payne JD, West JL. Cancer Lett. 2004; 209:171–176. [PubMed: 15159019]
25. Wust P, Hildebrandt B, Sreenivasa G, Rau B, Gellerman J, Riess H, Felix R, Schlag PM. Lancet Oncol. 2002; 3:487–497. [PubMed: 12147435]

26. Chen J, Wang D, Xi J, Au L, Siekkinen A, Warsen A, Li ZY, Zhang H, Xia Y, Li X. Nano Lett. 2007; 7:1318–1322. [PubMed: 17430005]
27. Tong L, Zhao Y, Huff TB, Hansen MN, Wei A, Cheng J-X. Adv Mater. 2007; 19:3136–3141. [PubMed: 19020672]
28. Huff TB, Tong L, Zhao Y, Hansen MN, Cheng J-X, Wei A. Nanomedicine. 2007; 2:125–132. [PubMed: 17716198]
29. Niidome T, Akiyama Y, Shimoda K, Kawano T, Mori T, Katayam Y, Niidome Y. Small. 2008; 4:1001–1007. [PubMed: 18581412]
30. Chanda N, Shukia R, Katti KV, Kannan R. Nano Lett. 2009
31. Chmberland DL, Agarwal A, Kotov N, Fowlkes JB, Carson PL, Wang X. Nanotechnology. 2008; 19:1–7. [PubMed: 19436766]
32. Sönnichsen C, Franzl T, Wilk T, von Plessen G, Feld-mann J. Phys Rev Lett. 2002; 88:077402. [PubMed: 11863939]
33. Imura K, Nagahara T, Okamoto H. J Phys Chem. 2005; 109:13214–13220.
34. Pelton M, Liu M, Kim HY, Smith G, Guyot-Sionnest P, Scherer NF. Opt Lett. 2006; 31:2075–2077. [PubMed: 16770437]
35. Liao H, Hafner JH. Chem Mater. 2005; 17:4636–4641.
36. Niidome T, Yamagata M, Okamoto Y, Akiyama Y, Takahashi H, Kawan T, Katayama Y, Niidome Y. J Controlled Release. 2006; 114:343–347.
37. Takahashi H, Niidome Y, Niidome T, Kaneko K, Kawasaki H, Yamada S. Langmuir. 2006; 22:2–5. [PubMed: 16378388]
38. Eghtedari M, Liopo AV, Copland JA, Oraevsky AA, Motamedi M. Nano Lett. 2008; 9:287–291. [PubMed: 19072129]
39. Wang C, Chen J, Talavage T, Irudayaraj J. Angew Chem Int Ed. 2009; 48:2759–2763.
40. El Sayed IH, Huang X, El Sayed MA. Nano Lett. 2005; 5:829–834. [PubMed: 15884879]
41. Rouhana LL, Jaber JA, Schlenoff JB. Langmuir. 2007; 23:12799–12801. [PubMed: 18004894]
42. Carb-Argibay E, Rodrguez-Gonzlez B, Pacifico J, Pastoriza-Santos I, Perez-Juste J, Liz-Marzan LM. Angewandte Chemi International Edition. 2007; 46:8983.
43. Perez-Juste J, Pastoriza-Santos I, Liz-Marzan LM, Mulvaney P. Coordination Chem Reviews. 2005; 249:1870.
44. Smith DK, Miller NR, Korgel BA. Langmuir. 2009; 25:9518–9524. [PubMed: 19413325]
45. Grzelczak M. Adv Funct Mater. 2008; 18:3780–3786.
46. Ha TH, Koo HJ, Chung BH. J Phys Chem C. 2007; 111:1123.
47. Niidome T, Yamagata M, Okamoto Y, Akiyama Y, Takahashi H, Kawano T, Katayama Y, Niidome Y. J Control Release. 2006; 114:343–347. [PubMed: 16876898]
48. Storm G, Belliot SO, Daemen T, Lasic DD. Adv Drug Delivery Rev. 1995; 17:31–48.
49. Dunn SE, Brindley A, Davis SS, Davis MC, Illum L. Pharm Res. 1994; 7:1016–1022. [PubMed: 7937542]

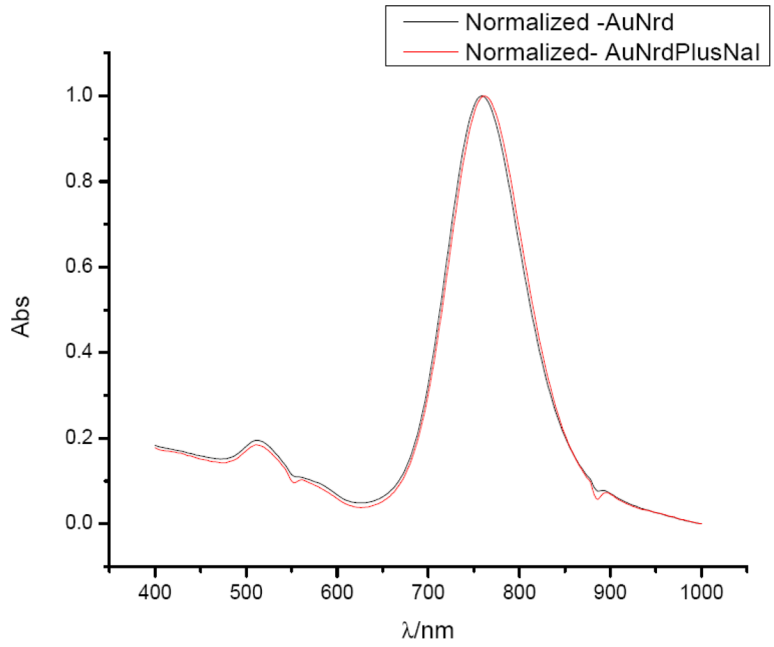

Figure 1.
UV-Vis of gold nanorods before and after labeling with I-125

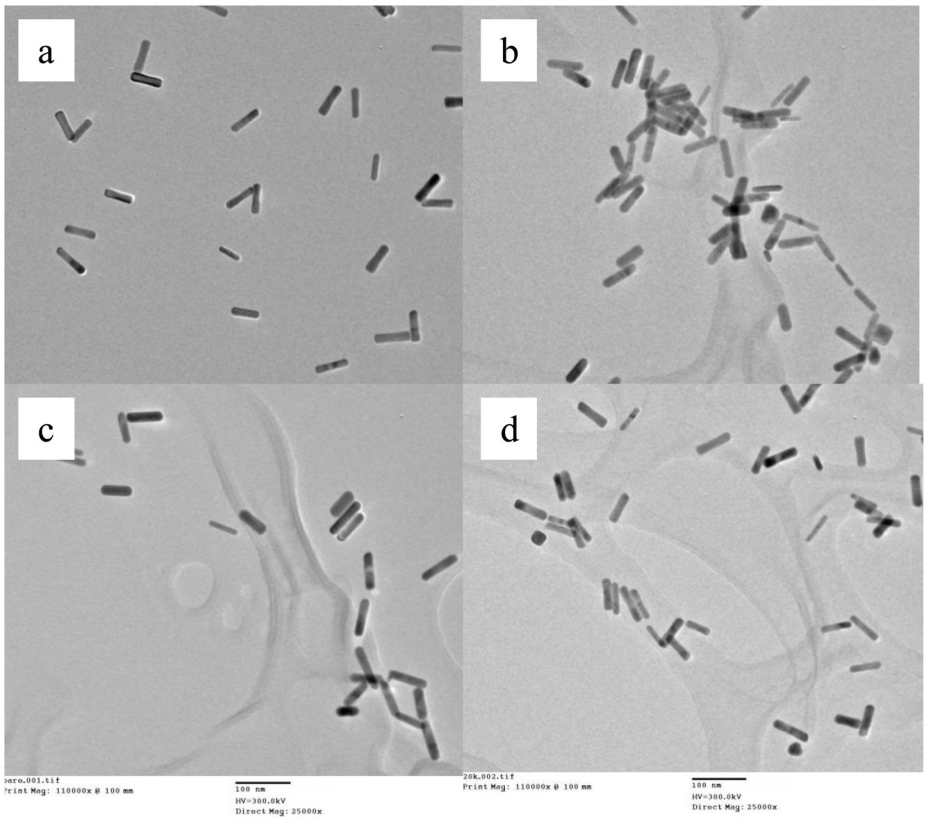

Figure 2.
TEM images of bare GNRs (a), bare GNRs with I-125 (b), PEGylated GNRs (c), and PEGylated GNRs with I-125(d).

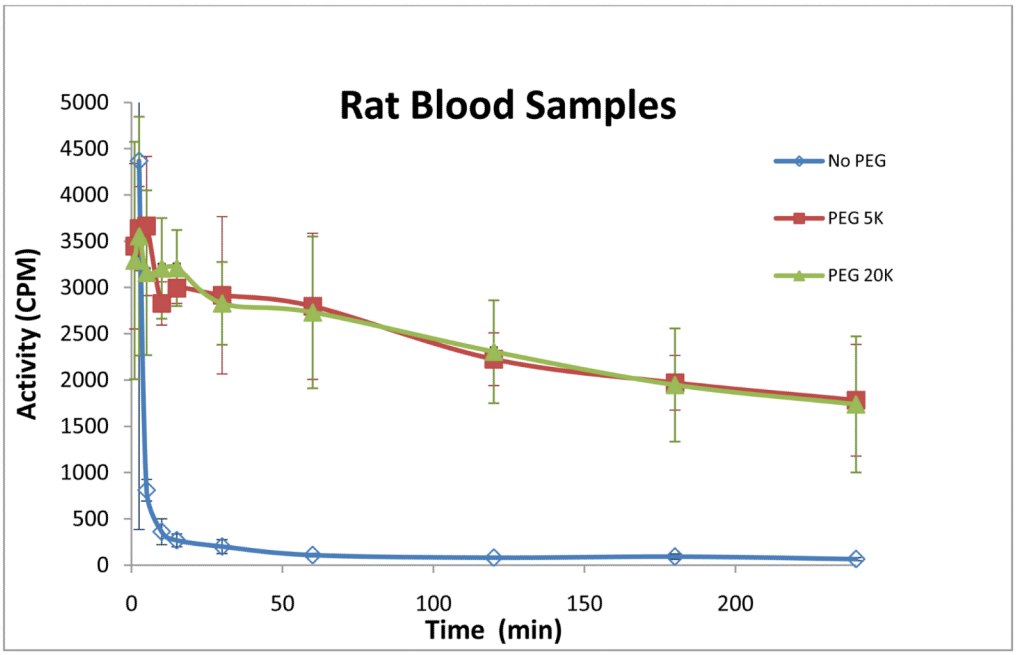

Figure 3.
Blood time-activity curves

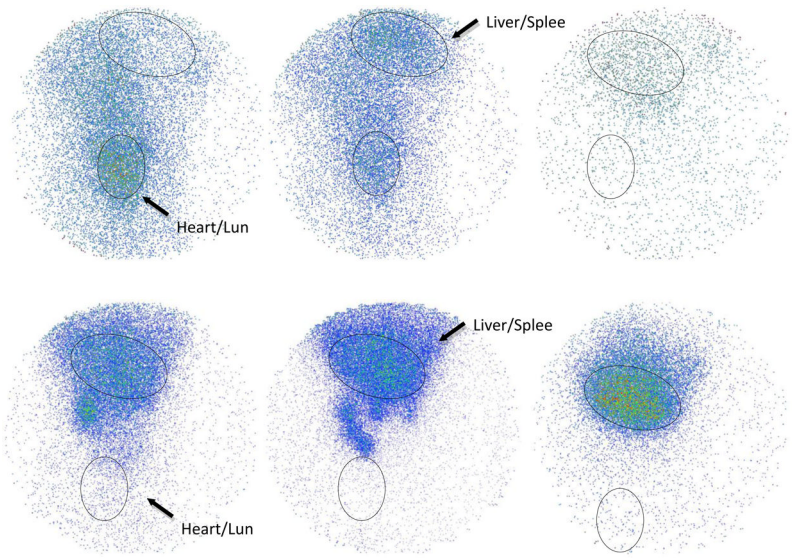

Figure 4.
Gamma images at different post-injection time (5 min, 4 hr, 6 day). The upper three images are from a rat injected with PEGylated GNRs. The lower three images are from a rat injected with bare GNRs.

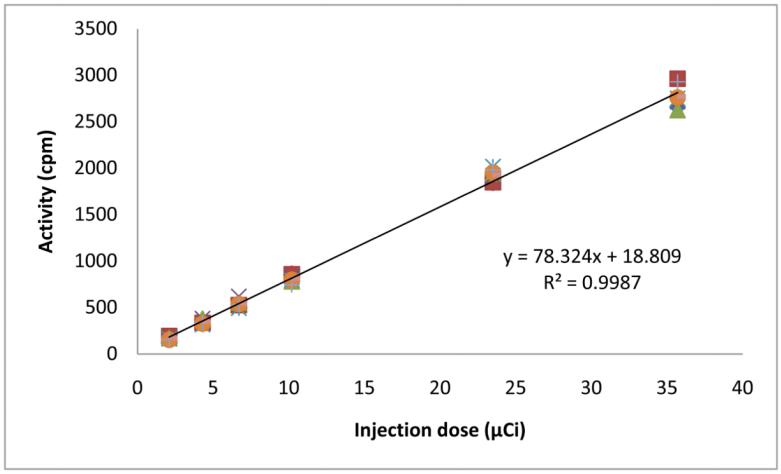

Figure 5.
^{125}I-GNRs standard curve

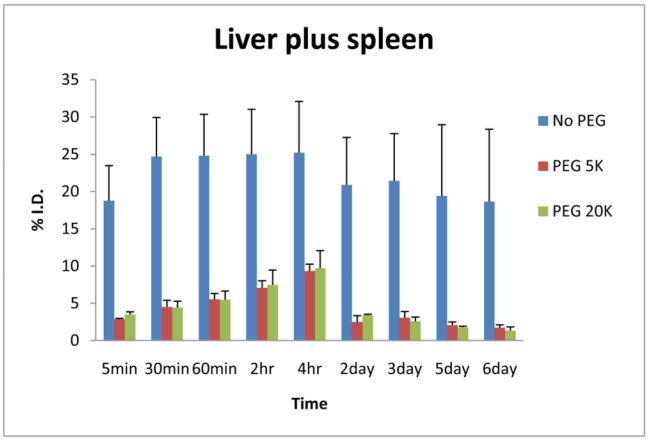

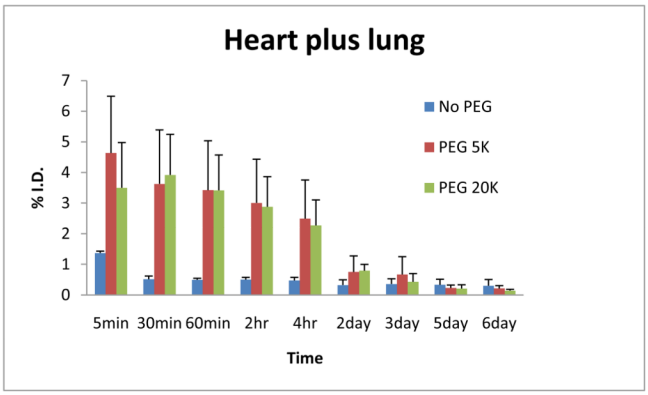

Figure 6.
Activities in liver/spleen and heart/lung vs. time

Table 1

Summary of centrifugation for various periods

Total time (min)	Radioactivity in pellets (% from total, n = 12)	Aggregation (%) n = 12
5	60.0 ± 6.1	0
10	74.4 ± 3.3	0
15	90.0 ± 3.1	0
30	99.4 ± 0.6	33.3